DOI: 10.15825/1995-1191-2022-4-60-72

TREATMENT OF CHRONIC LIVER DISEASE USING CELL-ENGINEERED CONSTRUCTS: MORPHOFUNCTIONAL CHARACTERISTICS

M.Yu. Shagidulin[1, 2], N.A. Onishchenko[1], A.V. Grechina[2], M.E. Krasheninnikov[4], A.O. Nikolskaya[1], E.A. Volkova[1], N.P. Mogeiko[1], N.A. Boiarinova[2], A.V. Lyundup[4], G.A. Piavchenko[2], L.I. Davydova[3], A.Yu. Arhipova[5, 6], V.G. Bogush[3], S.V. Gautier[1, 2]

[1] Shumakov National Medical Research Center of Transplantology and Artificial Organs, Moscow, Russian Federation
[2] Sechenov University, Moscow, Russian Federation
[3] Kurchatov Institute, Moscow, Russian Federation
[4] RUDN University, Moscow, Russian Federation
[5] Moscow State University, Moscow, Russian Federation
[6] Shenzhen MSU-BIT University, Shenzhen, China

Objective: to study the effectiveness of correcting the morphofunctional characteristics of the liver in an experimental model of chronic liver disease (CLD), using implanted cell-engineered constructs (CECs). **Materials and methods.** Experiments were carried out on male Wistar rats (n = 80) aged 6–8 months with an initial weight of 230–250 g. CLD was modeled by inoculating the rats with 60% CCl_4 oil solution for 42 days based on a modified scheme. Microgel based on recombinant spidroin rS1/9 was used as a matrix for CECs fabrication. Allogeneic liver cells (LCs) and multipotent bone marrow-derived mesenchymal stem cells (BM-MSCs) from a healthy donor were used as the cellular component of the CECs. The effectiveness of the corrective effect of the implanted CECs was assessed in an experimental CLD model (n = 60) in two groups of rats: Group 1 (control, n = 20, 1 mL of saline solution was injected into the damaged liver parenchyma) and Group 2 (experimental, n = 40, CECs containing allogenic LCs and BM-MSCs in a 5 : 1 ratio in a volume of 1 mL were implanted into the damaged liver parenchyma). For long-term monitoring of the CEC state, the CECs were labeled by additional inclusion in Cytodex-3. The effectiveness of the regulatory effect of CECs on regenerative processes in the liver was evaluated using biochemical, morphological and morphometric techniques, as well as by flow cytometry at 90 days after implantation. **Results.** In the control group, the mortality rate in CLD was 25%. There was no death in the experimental group with CLD after CEC implantation. The CECs were found to have a corrective effect on the biochemical and morphological parameters of the liver in CLD during 90 days of follow-up, with concomitant preservation of structural cellular homeostasis in the implanted CECs. **Conclusion.** Implantation of CECs in the liver facilitates effective correction of CLD by activating regenerative processes in the damaged liver, which is due to long-term preservation of structural cellular homeostasis in the CECs.

Keywords: regenerative medicine, chronic liver disease treatment, matrix, microgel, liver cells, bone marrow-derived mesenchymal stem cells, cell-engineered constructs.

INTRODUCTION

Over the past decades, Russia and the world at large have witnessed a significant increase in the number of severe chronic liver disease (CLD), leading to decompensated CLD. The disease is progressive in nature, which requires continuous corrective actions. Among the treatment options, liver transplantation is the most effective and the only radical treatment for end-stage CLD with respect to long-term survival of patients [1, 2].

The main goal of the current stage of transplantology is to ensure that all patients in need have access to organ transplantation. The need for liver transplantation is 20 per million population [1]. However, the progressively growing shortage of donor organs limits the use of this high-tech form of care, so the number of patients on the waiting list continues to grow steadily [2–5]. The steady growth of chronic liver diseases [3], leading to irreversible damage, requires new effective methods of treatment.

Analysis of works carried out in the field of transplantology and artificial organs testifies to the emergence of a fundamentally new approach to the regenerative treatment of damaged vital organs, based on tissue engineering and regenerative medicine (TERM) [6].

Corresponding author: Murat Shagidulin. Address: 1, Shchukinskaya str., Moscow, 123182, Russian Federation. Phone: (499) 196-87-90. E-mail: dr.shagidulin@mail.ru

In connection with the above, developing biomedical technologies to support liver functions in patients with decompensated CLD and especially in patients on the liver transplant waitlist, is an urgent task for modern medicine [5].

One of the leading directions of TERM is the development of techniques for correction of affected liver functions in CLD by creating a new functionally active liver tissue that is capable of eliminating the deficiency in damaged liver functions for a certain period of time, especially in the pre-transplant period.

To date, a number of studies on the use of CECs, which included biopolymer-based scaffolds, LCs and multipotent BM-MSCs have been conducted [7, 8]. However, we did not find any studies on the application of recombinant spidroin microgel for the production of CECs for CLD correction and treatment.

Recombinant spidroin rS1/9 used in this work was created based on a protein whose gene was previously developed, synthesized and cloned in the Saccharomyces cerevisiae yeast cells [9]. rS1/9 is an analog of natural spidroin 1, one of the two proteins of dragline silk of the orb weaver spider *Nephila clavipes*, and characterized by molecular weight of 94 kDa and isoelectric point of pI = 10.3, i.e. it is positively charged at all pH values. In in vitro and in vivo experiments, rS1/9-based 2D and 3D materials/products have been shown to be characterized by absence of toxicity and allergenicity, slow resorption in the animal body, and ability to support adhesion and proliferation of different cell types [10]. A hydrogel was formed from a solution of recombinant spidroin rS1/9, from which a microgel was obtained by mechanical crushing, which is a suspension of microgel particles ranging from 100 to 300 μm in size, having a pronounced regenerative effect [11].

Objective: to, on an experimental CLD model, investigate the possibility of long-term correction and restoration of liver function by implantation of a CEC that is based on rS1/9 microgel containing allogenic LCs and BM-MSCs.

MATERIALS AND METHODS

To solve the tasks, experimental studies were carried out on male Wistar rats (n = 80) aged 6–8 months with an initial weight of 230–250 g. The animals were kept in a vivarium at a temperature of 18–20 °C on a mixed diet with free access to water. Experiments on animals were carried out from 9 am to 7 pm at room temperature (t = 22–24 °C), which excluded daily fluctuations in the mitotic activity in the liver cells; the relative humidity was 50–65%, the lighting cycle was twelve hours, and the change in room air volume per hour was tenfold. The diet at the vivarium for rats was standard: animals were fed a combined diet for laboratory animals (microbiological status complied with GOST R 51849-2001 "Veterinary and sanitary standards and requirements for the quality of feed for nonproductive 55 animals"), *ad libitum* filtered tap water was delivered in standard drinking bottles (microbiological status of water complied with SanPiN 2.1.4.1074-01 "Hygienic requirements for water quality in centralized drinking water supply systems"). Experiments and all manipulations with animals were performed according to the rules adopted in the European Convention for the Protection of Vertebrate Animals Used for Experimental and other Scientific Purposes (ETS 123), Strasbourg, 1986).

CLD was simulated by prolonged inoculation of male Wistar rats with carbon tetrachloride for 42 days according to the modified scheme [8].

The donors of allogenic LCs and BM-MSCs were male Wistar rats aged 5–6 months, weighing 150–230 g.

The cells were isolated and cultured in accordance with the general principles of culture studies. BM-MSCs were prepared according to the generally accepted procedure [8].

LCs were also prepared and used according to a known technique [12].

In the manufacture of CECs, isolated LCs ($2.5–4.0 \times 10^6$ cells/cm^3) and BM-MSCs ($0.5–0.8 \times 10^6$ cells/cm^3) were first co-cultured for 3 days using a certain ratio of these cells (LCs : BM-MSCs = 5 : 1). An additional 150 μL of rS1/9-based microgel suspension was added to the culture of co-cultured cells for their adhesion, and Cytodex-3 (150 μl volume) was added to enable assessment of the status of the cellular material in the CEC composition for long periods after implantation into the liver.

On day 7 after inoculation, the rats that survived CLD modeling (n = 60) were divided into 2 groups. Group 1 (control, n = 20, saline (CLD + 1.0 mL of saline solution) saline was injected into liver parenchyma). Group 2 (experimental, n = 40, CECs consisting of rS1/9 microgel, allogeneic LCs and BM-MSCs = 5 : 1, and 1 ml Cytodex-3 were injected into the liver parenchyma by chipping.

Yeast cultivation, isolation and purification of recombinant rS1/9 spidroin, preparation of hydrogel and microgel based on it were performed as previously described in accordance with a previously published protocol [11].

The morphology of the hydrogel surface was analyzed using a CamscanS2 microscope (Cambridge Instruments, UK). Images were obtained using MicroCapture software (SMA, Russia).

Adequacy control of the created CLD models and efficacy of correction of morphofunctional disorders in the liver using CECs was estimated according to mortality and survival of animals, morphological and morphometric characteristics of the liver, as well as CECs themselves. The functional efficacy of CECs was assessed based on biochemical blood parameters. After modeling CLD and the therapy used, the surviving animals were removed from the experiment at day 90 by

intraperitoneal injection of sodium thiopental in a dose causing respiratory arrest. At autopsy, liver biopsies were subjected to morphological and morphometric studies. Immunosuppression was not used.

Live blood sampling from rats for biochemical studies was performed under ether anesthesia by notching the tip of the tail. Liver function – alanine aminotransferase (ALT), aspartate aminotransferase (AST), alkaline phosphatase (ALP) – was studied on a Reflotron™ biochemical analyzer (Roche, Switzerland) using special Reflotron test strips.

For morphological studies, we used liver from groups 1 and 2 animals. We studied the state of regenerative processes in the liver both inside and outside the CEC implantation areas. We evaluated light microscopy data by staining the sections with hematoxylin and eosin, Mallory and Van Gieson (Leica DM 6000 B microscope with Leica LTDCH 9435 camera, Germany).

Morphometric analysis was performed using morphometric software ImageScopeM (Systems for microscopy and analysis, Russia) using a Leica DM 1000 microscope and a Leica LTDCH 9435 DFC 295 camera (LeicaCamera AG, Germany). We determined morphometrically the following: the presence of cirrhosis (counting the number of false lobules); specific area of connective tissue (in % of the total area of liver section) [13, 14]; we counted the number of binuclear hepatocytes (per 10 fields of view at 400× magnification), hepatocytes with signs of fatty A distinctly positive trend in the recovery of hepatic parenchyma was noted. Liver architectonics was almost completely restored, regression in fatty degeneration and its transition to a fine-droopy form was noted; liver lobule structure was restored. Preserved hepatocytes without signs of dystrophy around the veins appeared; beam architectonics was restored, formation of false lobules was not determined (Fig. 3, g), whereas in the control, there were appearance of false lobules and expressed protein degeneration of hepatocytes, sclerosis and fibrosis of liver parenchyma, hepatocytes with degenerating nuclei and intranuclear lipid inclusions; area of blood vessels and bile ducts (in ‰).

For verification and structural analysis of liver tissue slices, images were processed using artificial intelligence (AI) analysis. This method is an effective way to analyze and present results obtained [15, 16] and allows to clearly differentiate structures in the tissue based on tinctorial properties.

MATLAB program (MATLAB Corporation, USA) was used to transform images of liver histological sections into three-dimensional space. The following types of structures were distinguished: “oxyphilic hepatocyte cytoplasm”, “basophilic hepatocyte nuclei”, “fibrous connective tissue”, “intercellular substance” and “empty spaces (vascular lumen, adipocytes)”. The initial image was converted to grayscale. After that, a 3D model was built taking into account the added constants for each grayscale image. Constructed models and pseudocoloring were individualized for each image [17].

Methylene blue staining was used for assessing cell viability in the primary culture [18].

The blood levels of CD4+CD25+Foxp3+ Tregs, which reflects the degree of immune tolerance to allogeneic cells in CECs, was also measured using flow cytometry (BeckmanCoulter, USA). For this purpose, blood lymphocytes were labeled with rat $CD4^{+}CD25^{+}Foxp3^{+}$ antibodies from eBioscience (USA).

Results obtained were statistically processed using the computer statistical package Biostat; the significance of differences was assessed by Student’s t-test with Bonferroni correction taken into account. Differences were considered significant at $p < 0.05$ (statistical package recommended by WHO, EpiInfo 5.0). Actuarial survival of animals within one year after CLD modeling (control) and against its correction by CECs implantation was calculated according to Kaplan–Meier using statistical software package Statistica for Windows, v.12.

RESULTS

The viability of the primary culture of BM-MSCs was 94 ± 2%. Cell suspension prepared from donor liver contained ~95–98% hepatocytes and ~5–2% non-parenchymal cells; they had 76 ± 4% viability. The cells were not separated into parenchymal and non-parenchymal.

The structure of the microgel surface was analyzed by scanning electron microscopy (SEM). The microgel represents microparticles with an average size of 100 to 300 μm and a pronounced relief surface; the surface elements of the hydrogel include nanostructures of 100 to 300 nm in diameter and microstructures of 10 to 30 μm in size (Fig. 1).

After obtaining the primary cell culture, we considered it necessary to pre-culture them to eliminate stress damage during isolation and activate their cellular functions. For this purpose, BM-MSCs were cultured for 7 days and then co-cultured with LCs introduced into the culture for subsequent 3 days. The cells were co-cultured not only in a stationary mode but also in a rotational mode (1.5–2.0 rpm) to simulate mass exchange provided by blood circulation, because only under these conditions can there be long-term viability and proliferative activity of LCs when co-cultured with BM-MSCs. To determine the suitability of rS1/9 for LCs adhesion, studies were performed that confirmed active LCs adhesion on the rS1/9 surface.

Mortality was 25% during CLD modeling. Further, after inoculation in the control group (group 1), animals continued to die: 5 rats died out of 20 (25%), which, in our opinion, confirms the adequacy of the chosen CLD model. In the experimental group (group 2), there was no mortality at this time point (day 90). Actuarial survival at the inoculation stage and during treatment is shown in Fig. 2, a and b.

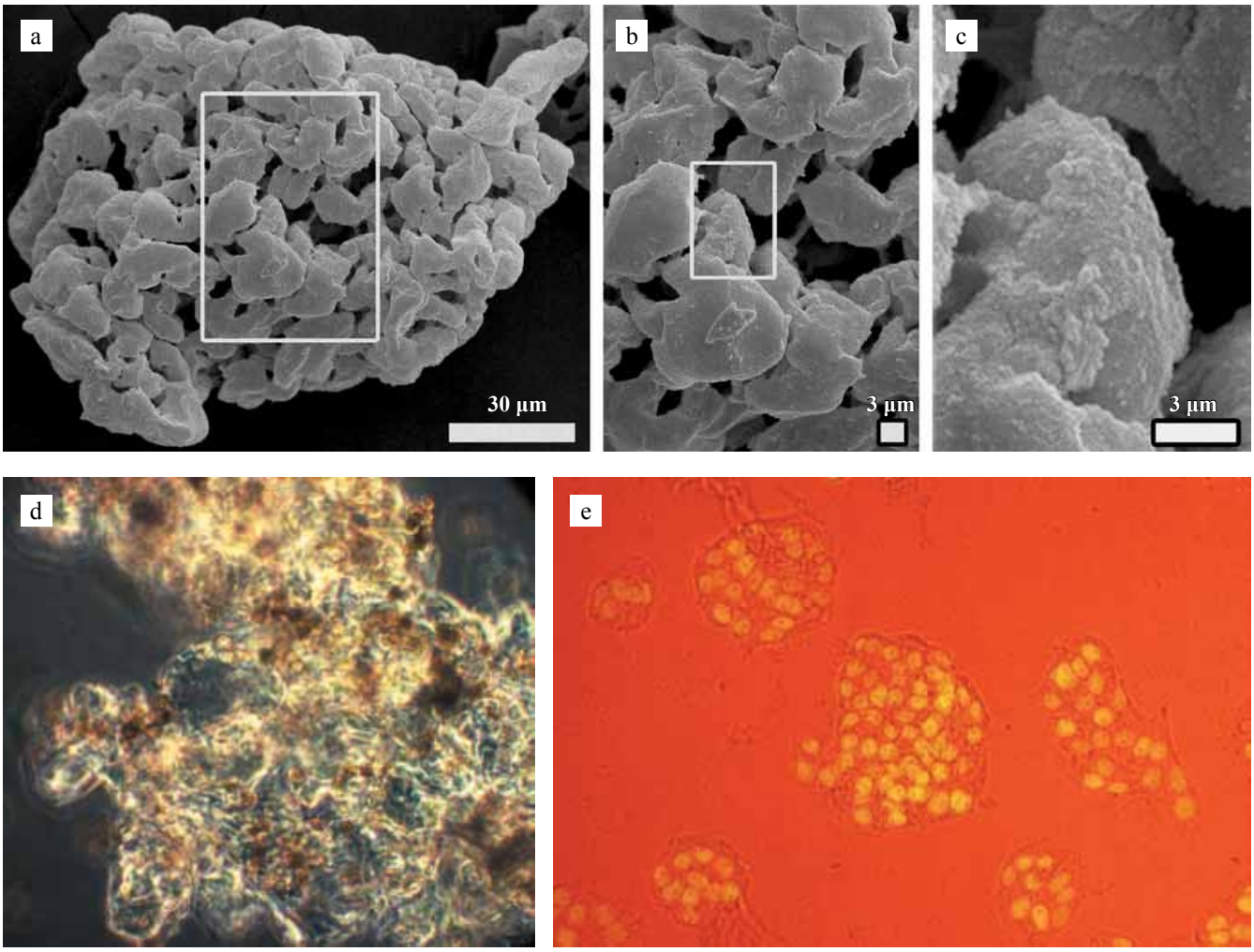

Fig. 1. Structure of rS1/9-based microgel: a, SEM image of microgel particle (scale bar = 30 µm); b and c, enlarged image of the area in a white frame (scale bar = 3 µm); d, Co-cultivation of LCs and BM-MSCs on rS1/9, phase contrast microscopy images (400× magnification); e, Staining for specific hepatocyte nuclear antigen 4 (HNF-4), fluorescence microscopy + phase contrast (200× magnification)

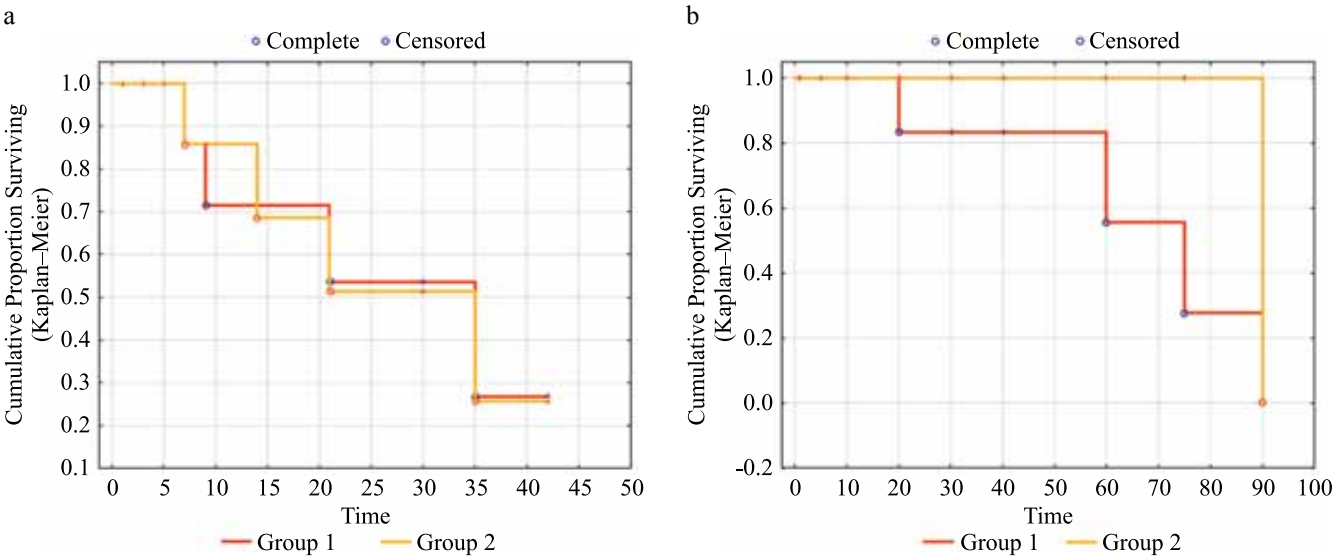

Fig. 2. Actuarial survival (according to Kaplan–Meier estimate): a, during CLD modeling: Gehan's Wilcoxon Test (Spreadsheet1) WW = –1,000 Sum = 670.00 Var = 76.32 Test statistic = –0.037655 p = 0.96996, and b, during CLD treatment: Gehan's Wilcoxon Test (Spreadsheet1) WW = –11.00 Sum = 238.00 Var = 62.632 Test statistic = –1.32676 p = 0.18459

At the initial stage of the study, the normal structure of the liver tissue was studied. Homogeneous liver parenchyma formed by hepatic cord of hepatocytes (D), with sinusoidal capillaries located between them in the form of slit-like spaces was revealed; the presence of endothelium and capillary and vein lumen was detected (Fig. 3, a–c).

After inoculation (42 days), on day 7 the following was revealed: changes in the beam structure of liver lobules, pronounced polymorphism of parenchymal cells, fatty degeneration in hepatocytes, karyorrhexis, karyolisis, hepatocyte necrosis. Massive fatty degeneration in hepatocytes and formation of false lobules were detected (Fig. 3, d–f).

By day 90 after CLD modeling, the control group witnessed subtotal restructuring of liver histoarchitectonics with replacement of normal parenchyma by false lobules. Sclerotic changes (fibrosis) were manifested by the formation of collagen fibers along the portal tracts and formation of porto-portal and porto-central septa with the formation of false lobules. Focal hepatocyte necroses, enlargement and plethora of sinusoids and plethora of central veins were revealed. Rare lymphoid-cell infiltration, proliferation of histioblasts and histocytes were noted in the liver parenchyma. In the experimental group, by day 90, we observed significantly less severity of toxic liver damage compared with the control. A distinctly positive trend in the recovery of hepatic parenchyma was

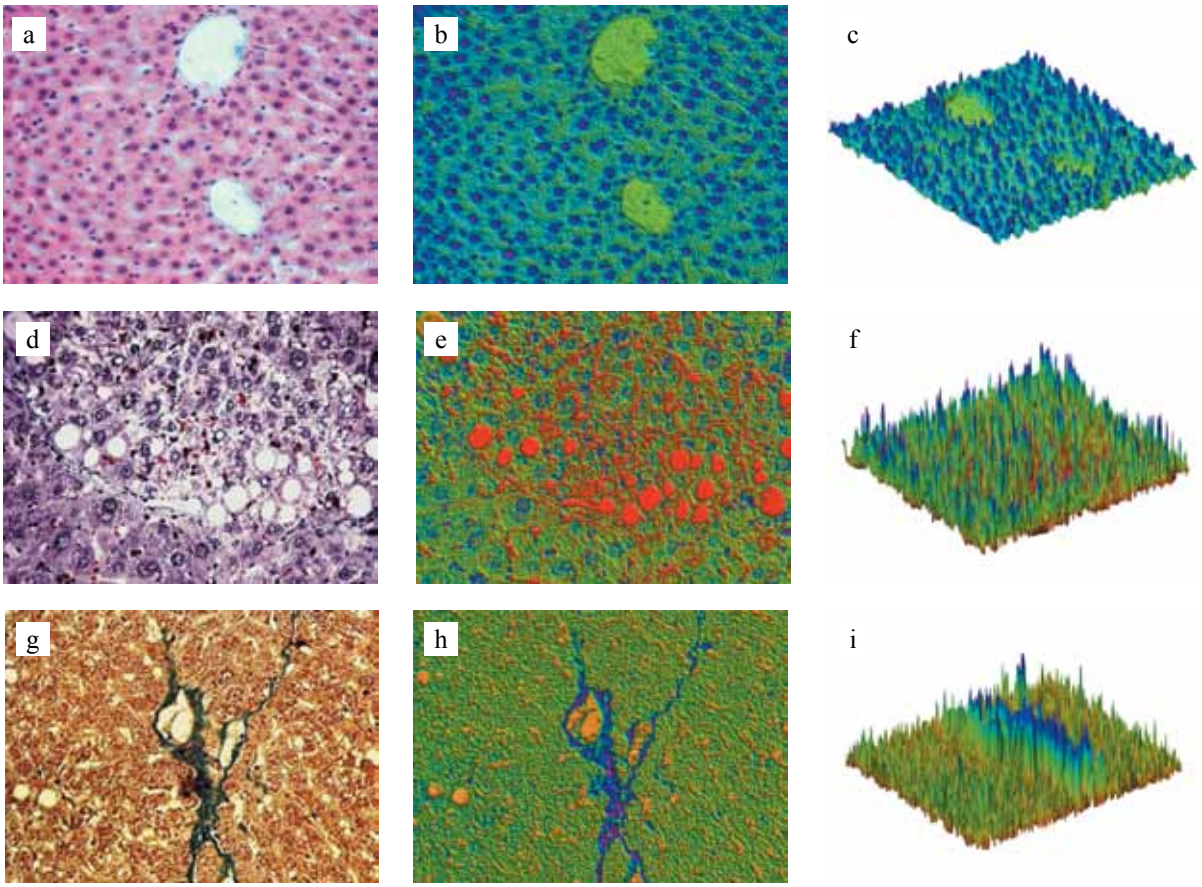

Fig. 3. Histological and pseudostained 2D and 3D liver preparations: a, Tissue specimens of healthy liver: Central part of the lobule with preserved structures with the presence of two central veins. Balloon structure is not disturbed, granular hepatocyte dystrophy, slight expansion of sinusoids. H&E staining (200× magnification). b, c, Pseudo-stained 2D and 3D images revealed the general structure of organ parenchyma without pathological changes. Hepatocytes with oxyphilic staining of cytoplasm and basophilic nuclei and a normal nuclear-cytoplasmic ratio, sinusoidal capillaries were not dilated. Hepatocyte cytoplasm is pseudostained in blue, nuclei are blue, sinusoidal spaces and vascular lumen are green, basophilic hepatocyte nuclei are lilac. d, Liver tissue specimen on day 7 after the end of CLD modeling: initial formation of fibrous tissue, focal proteinaceous granular degeneration of hepatocytes, significant group of cells in a state of ballooning degeneration and necrosis. Focal large- and small-drop fatty degeneration in hepatocytes. Sinusoidal dilatation and plethora. Rare lymphoid-cell infiltration in the parenchyma. Van Gieson's staining (400× magnification; e, f, Fatty degeneration of hepatocytes with a shift in nuclear-cytoplasmic ratio: hepatocytes with increased volume of cytoplasm. Areas of fibrosis are identified. On pseudo-stained 2D and 3D (e, f) images, hepatocyte cytoplasm is green, hepatocyte nuclei are blue and purple for pronounced hyperchromic tinctorial properties. Red color for empty spaces, predominantly in hepatocytes with fatty degeneration. g, Liver tissue specimen at day 90: CLD + CEC implantation with LCs and BM-MSCs (group 2). Central part of the lobule with preserved structures. Van Gieson's staining (200× magnification). In Fig. 3, h and i, hepatocyte cytoplasm is green, their nuclei are blue and purple with pronounced tinctorial properties, the prevailing empty spaces in hepatocytes with fatty degeneration are red

noted. Liver architectonics was almost completely restored, regression in fatty degeneration and its transition to a fine-droopy form was noted; liver lobule structure was restored. Preserved hepatocytes without signs of dystrophy around the veins appeared; beam architectonics was restored, formation of false lobules was not determined (Fig. 3, g), whereas in the control, there were appearance of false lobules and expressed protein degeneration of hepatocytes, sclerosis and fibrosis of liver parenchyma.

To objectify the results obtained, we performed quantitative and semi-quantitative assessment of structural changes occurring in the liver tissue in CLD without treatment and with the use of CECs. We performed morphometric studies of liver parenchyma cells (counting the number of hepatocytes with signs of fatty degeneration, with degenerating nuclei, with intranuclear lipid inclusions and counting the number of binucleated hepatocytes); as well as non-parenchymal structures (determination of the connective tissue specific area and the number of false lobules in liver), including blood vessels and bile ducts area in the liver tissue at day 90 after CLD modeling (Fig. 4, a, b).

A morphometric study of the state of non-parenchymal structures (determination of the specific area of the connective tissue and the number of false lobules in the liver) for a period of 90 days showed that under the influence of CECs, liver parenchyma was restored, the specific area of the liver connective tissue reduced (Fig. 4, a) and the number of false lobules in it also reduced (Fig. 4, b). At the same time, the control group showed an increase in these indicators – 8.2% and 2.8%, respectively.

It was also found that treatment with CECs (experimental group 2) resulted in a rapid and significant decrease in the number of hepatocytes with signs of fatty degeneration, with degenerating nuclei, with intranuclear lipid inclusions and a more pronounced significant increase in the number of binuclear hepatocytes. Moreover, the above changes were combined with a pronounced positive clinical effect. At day 90, blood vessel and bile duct area in the liver tissue normalized in comparison with the control group (Fig. 4, c–h).

The above studies suggest that regenerative processes in both non-parenchymal and parenchymal structures of liver tissue in CLD are intensified only when CECs are used with allogeneic LCs and BM-MSCs.

The identified features of liver regeneration when CECs are used with allogeneic LCs and BM-MSCs made it necessary to study the histological state of the CECs themselves and the surrounding liver tissue at day 90 after implantation.

Obtained results indicate that allogeneic LCs in CECs implanted into the recipient liver retain their viability and proliferative activity for a long time (90 days), with no signs of rejection, despite the absence of immunosuppression (Fig. 5, a–f).

Histological and model three-dimensional analysis of the state of hepatocytes in CECs implanted into the liver parenchyma in CLD showed that structural changes in hepatocytes in CECs are well distinguishable in tissue specimens. They are clearly identified by different color staining, which allows different structures to be distinguished. Thus, implantation of CECs containing rS1/9-based microgel and allogeneic LCs and BM-MSCs leads to positive structural changes in the liver parenchyma on the background of long-term preservation, development and maintenance of normal structural homeostasis in hepatocytes within the CECs.

It can be assumed that the long-term absence of distinct signs of immune rejection of CECs containing allogeneic cells (LCs and BM-MSCs) is a consequence of local implementation of immunomodulatory and tolerogenic properties inherent in BM-MSCs, which protect CECs against immune rejection and allow them to function for long and efficiently.

A blood test for Tregs levels by flow cytometry confirmed that rats with CLD that are treated by implantation of CECs containing allogeneic LCs and BM-MSCs, as well as the healthy controls, maintained the initial blood level of $CD4^+CD25^+Foxp3^+$ Tregs after 90 days (Fig. 6, a–c).

At the same time, there was a significant increase in the content of this pool of Regulatory T cells in the experimental group by day 90 as compared to the control group. Results of the conducted studies suggest that maintenance of the viability of the transplanted allogeneic LCs and BM-MSCs in CECs for a long time is due to immunological tolerance in the body induced and maintained by BM-MSCs.

Parallel studies of the functional state of the liver by means of dynamic measurement of serum biochemical indicators confirmed the development of sustained toxic damage to the liver immediately after CLD modeling. Development of CLD was accompanied by severe impairment of liver functional indicators: ALT, AST and ALP – they sharply increased in groups 1 and 2 animals immediately within the first 7 days after inoculation. However, in the experimental group (with CECs implantation), during the first 30 days, the studied biochemical parameters (ALT, AST, ALP) normalized rapidly and recovered completely by the end of the observation period.

Upon further follow-up in the group with implanted CECs, biochemical parameters characterizing a cytolytic syndrome remained within normal limits; in the control group (group 1), these parameters remained elevated for 90 days. This explains 25% mortality in the control group in the study period.

Thus, rapid normalization of cytolytic syndrome enzymes, the histological structure of the damaged liver tissue, a more pronounced decrease in the specific area of connective tissue, as well as reduced number of hepatocytes with fatty regeneration and degenerating nuclei

in the rat liver tissue, at day 90 after the end of CLD modeling and use of CECs in the experimental group, allows us to state that the implanted rS1/9-based CECs, which include allogenic LCs and BM-MSCs in a 5 : 1 ratio, effectively modulate regenerative processes in the damaged liver tissue. This is obviously due to the long-term preserved morphofunctional homeostasis in the newly formed hepatitis-like structure of the CECs

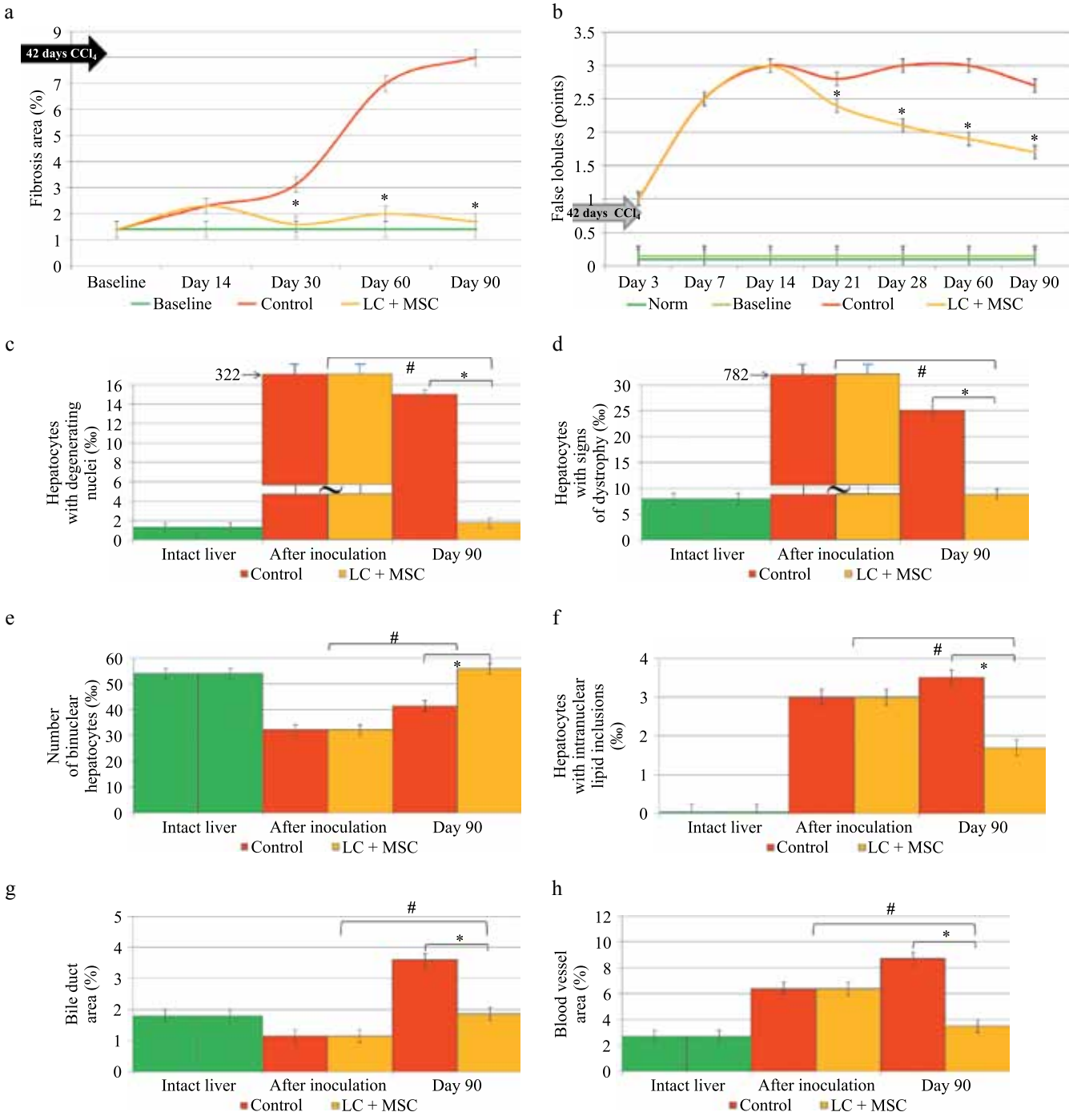

Fig. 4. Dynamic morphometric assessment of the state of nonparenchymal structures in CLD simulation without and with CEC implantation at day 90. a, Change in the specific area of the connective tissue (%). *In intact animals, the average value of the specific area of the connective tissue was 1.4%.* b, Change in the number of false lobules in the liver. *, The difference is significant compared to the level of this indicator in the liver of control rats (group 1); $p < 0.05$. c–h: dynamic morphometric assessment of the characteristics of rat liver hepatocytes, bile ducts and blood vessels in CLD simulation without and with CEC implantation at day 90: c, hepatocytes with degenerating nuclei; d, hepatocytes with fatty degeneration; e, binuclear hepatocytes; f, hepatocytes with intranuclear lipid inclusions; g, bile duct area; h, blood vessel area. group 1, control (saline); group 2, CEC with allogeneic LCs : BM-MSCs = 5 : 1. *, The difference is significant compared to the level of this indicator in the liver of control rats (group 1); $p < 0.05$. #, The difference is significant in comparison with the level of this indicator in the liver of rats after inoculation, $p < 0.05$

themselves, which is formed and maintained after CECs implantation by factors produced by the damaged liver into the body.

CONCLUSION

The study of the possibility of effective correction of morphofunctional disorders in the liver during CLD modeling using CECs implanted into the liver tissue showed that CECs made on the basis of rS1/9 microgel and containing allogeneic LCs and BM-MSCs in a 5 : 1 ratio, promote activation of regenerative processes in the damaged liver and restoration of its functional and morphological state: rapid normalization of the level of cytolytic enzymes in the blood, hepatocyte proliferation and reduction of connective tissue area in the liver. It was also found that throughout the entire period of observation in the structures of the implanted CECs, there was preservation of morphofunctional homeostasis of LCs included in their composition. The results of studies suggest that the cells included into the CECs become the centers of formation of newly formed and long-term functioning hematopoietic tissue which, by producing bioregulatory factors, activates and supports the repair processes in the damaged liver. Results obtained suggest that the long-term survival and functioning of allogeneic LCs in implanted CECs is due to the involvement of

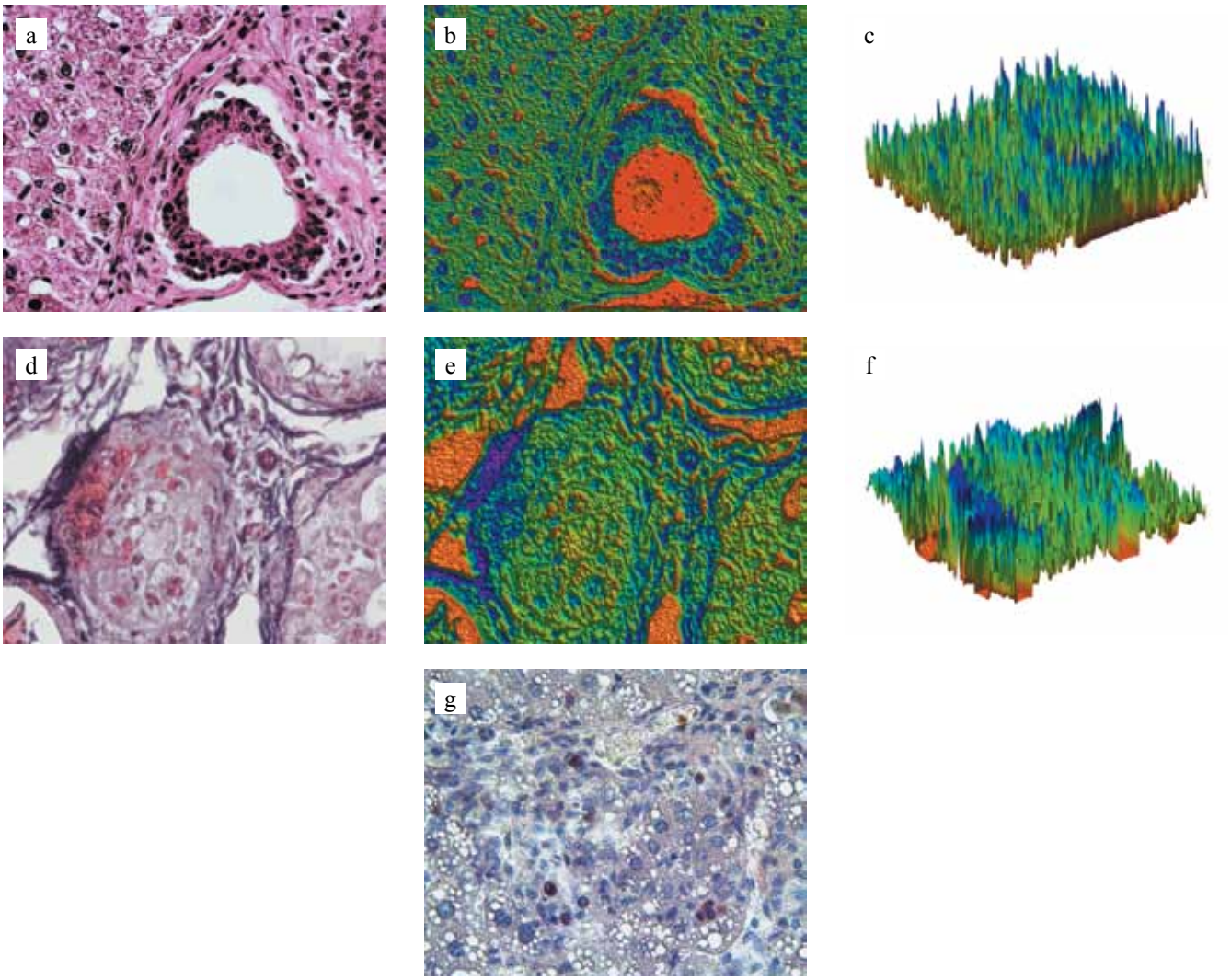

Fig. 5. Histological structure of hepatic CECs with allogeneic LCs and BM-MSCs (group 2) at day 90. a, transplanted hepatocytes as a part of CECs. H&E staining (400× magnification). b, c, there are structurally developing normal hepatocytes, hypertrophic hepatocytes, limited by fibrous connective tissue capsule, the shape and nuclear-cytoplasmic shifted to normal hepatocyte parameters. On the images after pseudo-coloring, the cell cytoplasm is green, nuclei are blue with purple inclusions, hepatocyte nuclei are in darker tones in a cell-engineered construct, the lumen is pseudo-stained red. d, transplanted hepatocytes as part of CECs. H&E staining (400× magnification; e, f, after destruction of the connective-tissue capsule, normal hepatocytes spread to neighboring areas and replace dystrophic hepatocytes. The fibrous connective tissue capsule disintegrates, and normal hepatocytes are located near its primary border. Images after pseudo-staining (e, f) show normal hepatocytes: cell cytoplasm is green, nuclei are blue, darker nuclei are purple in the cell-engineered construct, lumen is red. g, specifically PCNA-positive cells – light brown with dark brown nuclei, hepatocytes – oxyphilic cytoplasm and basophilic nuclei, PCNA staining by standard protocols with additional H&E staining (100× magnification)

BM-MSCs and rS1/9, contained in their composition, in maintaining the body's immune tolerance, due to which CECs are integrated into the damaged liver and symbiotically support each other.

Our studies have shown that implantation of CECs into the damaged liver creates numerous new centers for activation of repair processes. These centers were identified histologically and by three-dimensional analysis

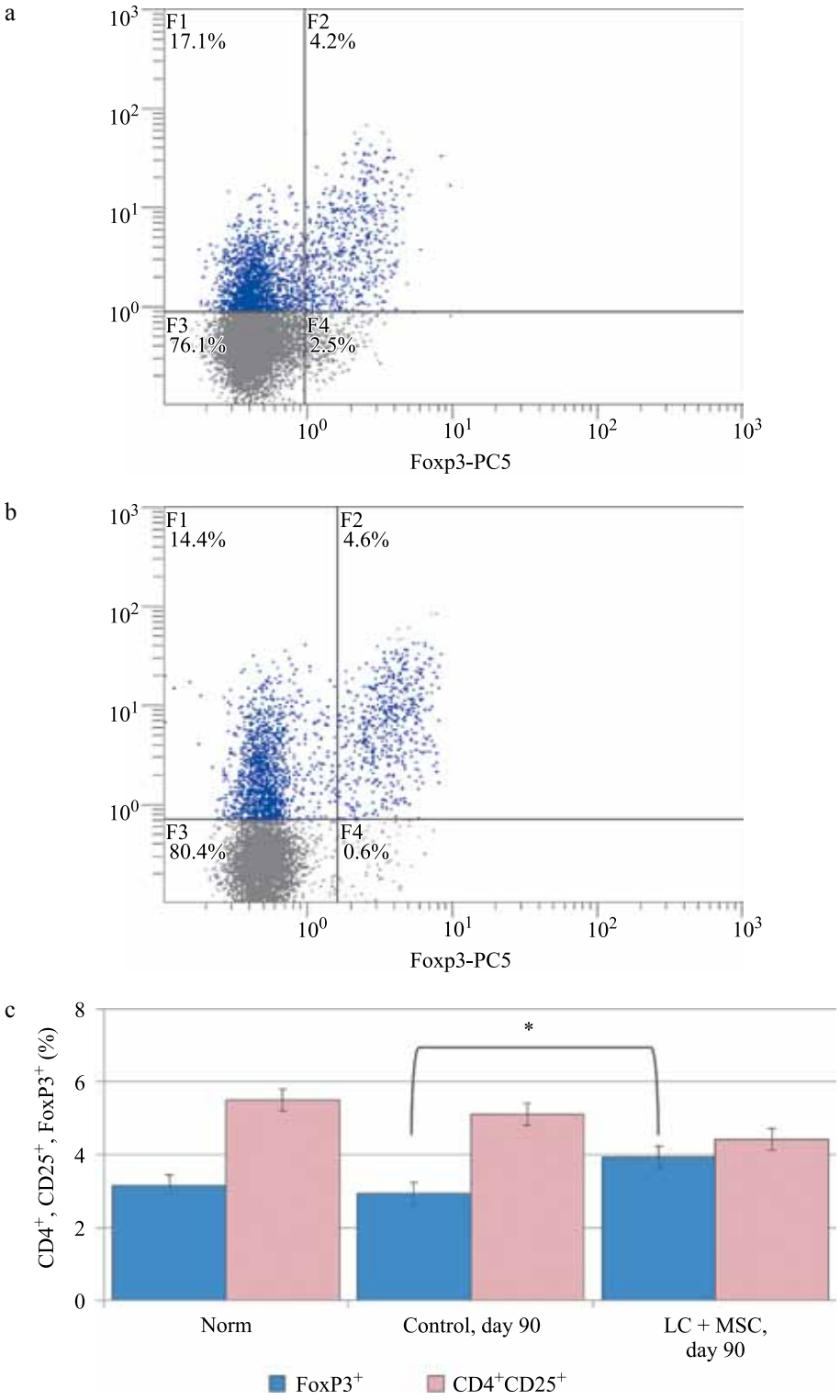

Fig. 6. Levels of $CD4^+CD25^+Foxp3^+$ Treg cells in the peripheral blood of rats: a, normal. b, day 90 after CLD modeling and implantation of CECs containing allogeneic LCs and BM-MSCs, experiments without immunosuppression. Flow cytometry. c, Graphical representation of levels of T lymphocytes containing CD4+, CD25+, Foxp3+ markers in peripheral blood of healthy, control rats after CLD modeling and implantation of CECs containing allogeneic LCs and BM-MSCs, in experiments at day 90 without immunosuppression (%). Flow cytometry. * $p < 0.05$ versus norm

of structural changes in the liver tissue and in CECs; the revealed positive structural changes in the liver were clearly visible in tissue specimens and were also identified by different color staining of structural elements of the liver in 2D and 3D images.

Implantation of CECs created on the basis of rS1/9 microgel and containing allogeneic LCs and BM-MSCs can become an effective method for correcting and treating CLD, and supporting damaged liver function in patients waitlisted for liver transplantation.

This work was supported financially by the Ministry of Science and Higher Education of the Russian Federation under Agreement No. 075-15-2021-1357.

The authors declare no conflict of interest.

REFERENCES

1. Transplantologija i iskusstvennye organy: uchebnik / Pod red. akad. RAN S.V. Gautier. M.: Laboratorija znanij, 2018; 319.
2. *Gautier SV, Konstantinov BA, Cirul'nikova OM.* Transplantacija pecheni. M.: MIA, 2008; 246.
3. *Mokdad A, Lopez A, Shahraz S, Lozano R, Mokdad A, Stanaway J et al*. Liver cirrhosis mortality in 187 countries between 1980 and 2010: a systematic analysis. *BMC. Med*. 2014; 12: 145. doi: 10.1186/s12916-014-0145-y.
4. World health statistics 2021: monitoring health for the SDGs, sustainable development goals World Health Organization, https: apps.who.int/iris/handle/10665/342703.
5. www.eurotransplant.nl/files/statistics.
6. *Atala A.* Building Organs for the Future. *Transplantation*. 2016; 100: 1595–15956. doi: 10.1097/TP.0000000000001301.
7. Metodicheskie rekomendacii po provedeniju doklinicheskih issledovanij biomedicinskih kletochnyh produktov / Pod red. akad. V.A. Tkachuka. M.: Moskovskij gosudarstvennyj universitet imeni M.V. Lomonosova, 2017; 256.
8. *Shagidulin MJu.* Razrabotka i jeksperimental'noe issledovanie kletochno-inzhenernyh konstrukcij pecheni dlja lechenija pechjonochnoj nedostatochnosti. [Dissertation]. M., 2015; 257.
9. *Bogush VG, Sokolova OS, Davydova LI et al.* A novel model system for design of biomaterials based on recombinant analogs of spider silk proteins. *J Neuroimmune Pharmacol*. 2009; 4 (1): 17–27. doi: 10.1016/j.biomaterials.2012.02.013.
10. *Debabov V, Bogush V*. Recombinant Spidroins as the Basis for New Materials. *ACS Biomater Sci Eng*. 2020; 6: 3745–3761. https: doi.org/10.1021/acsbiomaterials.0c00109.
11. *Nosenko MA, Moysenovich AM, Zvartsev RV, Arkhipova AY, Zhdanova AS, Agapov II et al*. Novel Biodegradable Polymeric Microparticles Facilitate Scarless Wound Healing by Promoting Re-epithelialization and Inhibiting Fibrosis. *Front Immunol*. 2018; 9: 2851. doi: 10.3389/fimmu.2018.02851. eCollection 2018.
12. *Gautier SV, Shagidulin MJu, Onishhenko NA, Krasheninnikov ME, Sevast'janov VI.* Sposob i transplantat dlja lechenija pechenochnoj nedostatochnosti. Patent № 2010110063/14(014141). 03.03.2011.
13. *Avtandilov GG*. Medicinskaja morfometrija: rukovodstvo. M.: Medicina, 1990; 384.
14. *Ishak K et al.* Gistologicheskaja ocenka stadii i stepeni hronicheskogo gepatita. *Klinicheskaja gepatologija*. 2010; 2: 8–11.
15. *Pradhan P, Guo S, Ryabchykov O, Popp J, Bocklitz TW.* Deep learning a boon for biophotonics? *J Biophotonics*. 2020; 13: e201960186. https://doi.org/10.1002/jbio.201960186.
16. *Rivenson Y, Wang H, Wei Z et al*. Virtual histological staining of unlabelled tissue-autofluorescence images via deep learning. *Nat Biomed Eng*. 2019; 3: 466–477. https://doi.org/10.1038/s41551-019-0362-y.
17. *Macenko M, Niethammer M, Marron JS, Borland D, Woosley JT, Guan X et al*. A method for normalizing histology slides for quantitative analysis. *2009 IEEE International Symposium on Biomedical Imaging: From Nano to Macro*. 2009: 1107–1110. doi: 10.1109/ISBI.2009.5193250.
18. *Godoy P, Hewitt NJ, Albrecht U, Andersen ME et al*. Recent advances in 2D and 3D in vitro systems using primary hepatocytes, alternative hepatocyte sources and non-parenchymal liver cells and their use in investigating mechanisms of hepatotoxicity, cell signaling and ADME. *Arch Toxicol*. 2013; 87 (8): 1315–1530. doi: 10.1007/s00204-013-1078-5.

The article was submitted to the journal on 17.05.2022